DMD Fast Forward. Published on June 18, 2007 as doi:10.1124/dmd.107.015909

DMD#15909

Stereoselective glucuronidation of 5-(4'-hydroxyphenyl)-5-phenylhydantoin by human UGT1A1, UGT1A9, and UGT2B15: effects of UGT-UGT interactions

Miki Nakajima, Hiroyuki Yamanaka, Ryoichi Fujiwara, Miki Katoh, and Tsuyoshi Yokoi

Drug Metabolism and Toxicology, Division of Pharmaceutical Sciences, Graduate School of Medical Science, Kanazawa University, Kanazawa, Japan

DMD Fast Forward. Published on June 18, 2007 as DOI: 10.1124/dmd.107.015909
This article has not been copyedited and formatted. The final version may differ from this version.

Running title: Stereoselective 4'-HPPH glucuronide formation

To whom all correspondence should be sent:

Tsuyoshi Yokoi, Ph.D.,

Drug Metabolism and Toxicology

Division of Pharmaceutical Sciences

Graduate School of Medical Science

Kanazawa University

Kakuma-machi, Kanazawa 920-1192, Japan

E-mail: tyokoi@kenroku.kanazawa-u.ac.jp

Tel / Fax +81-76-234-4407

This manuscript consists of 16 pages of text, 3 tables, 5 figures, and 24 references.

Abstracts: 225 words

Introduction: 396 words

Discussion: 813 words

[1]Abbreviations used are: CYP, cytochrome P450; UGT, UDP-glucuronosyltransferase; UDPGA, UDP-glucuronic acid; 4'-HPPH, 5-(4'-Hydroxyphenyl)-5-phenylhydantoin

DMD Fast Forward. Published on June 18, 2007 as DOI: 10.1124/dmd.107.015909
This article has not been copyedited and formatted. The final version may differ from this version.

Abstract

5-(4'-Hydroxyphenyl)-5-phenylhydantoin (4'-HPPH), a major metabolite of phenytoin in human, is exclusively metabolized to a glucuronide. 4'-HPPH has a chiral center. (*S*)-4'-HPPH is a predominant form produced from phenytoin in humans, and (*R*)-4'-HPPH is an extremely toxic form with respect to gingival hyperplasia. In the present study, we investigated the stereoselective 4'-HPPH *O*-glucuronide formation in human liver microsomes. Human liver microsomes predominantly formed (*S*)-4'-HPPH *O*-glucuronide rather than (*R*)-4'-HPPH *O*-glucuronide from racemic 4'-HPPH. Among human UDP-glucuronosyltransferase (UGT) enzymes, UGT1A1, UGT1A9, and UGT2B15 showed the 4'-HPPH *O*-glucuronide formation. Interestingly, UGT1A1 stereoselectively formed (*R*)-4'-HPPH *O*-glucuronide, whereas UGT1A9 and UGT2B15 stereoselectively formed (*S*)-4'-HPPH *O*-glucuronide from racemic 4'-HPPH. Using UGT1A double expression systems in HEK293 cells that we previously established, the effects of UGT-UGT interaction on 4'-HPPH *O*-glucuronide formation were investigated. It was demonstrated that coexpression of UGT1A4 increased the Vmax values of (*S*)- and (*R*)-4'-HPPH *O*-glucuronide formation catalyzed by UGT1A1, but decreased the Vmax values of (*S*)- and (*R*)-4'-HPPH *O*-glucuronide formation catalyzed by UGT1A9. Coexpression of UGT1A6 increased the S_{50} values and decreased the Vmax values of (*S*)- and (*R*)-4'-HPPH glucuronide formation catalyzed by UGT1A1 and UGT1A9. However, the interaction did not alter the stereoselectivity. In conclusion, we found that 4'-HPPH *O*-glucuronide formation in human liver microsomes is catalyzed by UGT1A1, UGT1A9, and UGT2B15 in a stereoselective manner, being modulated by interaction with other UGT1A isoforms.

Introduction

Phenytoin, 5,5-diphenylhydantoin, is a widely used anticonvulsant drug. It is metabolized to 5-(4'-hydroxyphenyl)-5-phenylhydantoin (4'-HPPH) mainly by cytochrome P450 (CYP) 2C9, and to a small extent, by CYP2C19 in humans (Giancarlo et al., 2001). 4'-HPPH has an asymmetric carbon atom. CYP2C9 preferentially catalyzes the formation of (*S*)-enantiomer of 4'-HPPH, whereas CYP2C19 is not stereoselective (Bajpai et al., 1996; Yasumori et al., 1999). It has been reported that 98% of circulating 4'-HPPH after phenytoin administration is (*S*)-enantiomer in humans (Yasumori et al., 1999; Ieiri et al., 1995). 4'-HPPH has no anticonvulsant properties, but is associated with side effects such as gingival hyperplasia, somnolence, dry month, and general fatigue (Ieiri et al., 1992). (*R*)-Enantiomer, although it is a minor metabolite, has been reported to be extremely toxic with respect to gingival hyperplasia (Ieiri et al., 1995). A number of studies suggest that 4'-HPPH is bioactivated by peroxidase to a free radical intermediate, which can oxidize lipids, proteins and DNA (Parman et al., 1998; Kim and Wells, 1996). However, 4'-HPPH is exclusively metabolized to glucuronide, which is a major metabolite of phenytoin in human (Yamanaka et al., 2005). Thus, glucuronidation is an important detoxification pathway of 4'-HPPH.

Glucuronidation of a variety of xenobiotics and endogenous compounds is catalyzed by UDP-glucuronosyltransferases (UGTs). In humans, the UGT superfamily of genes is divided into two families, *UGT1* and *UGT2*, based on sequence similarity at the amino acid level (Mackenzie et al., 2005). In our previous study, we found that 4'-HPPH O-glucuronide formation in human liver microsomes is catalyzed by UGT1A enzyme(s), although we could not determine which UGT1A enzymes make the major contribution (Nakajima et al., 2002). The limitation of the previous study was that the sensitivity was too low to detect the activity by recombinant UGTs. In our recent study, we improved the assay procedure and the HPLC condition to increase the sensitivity for the detection of 4'-HPPH *O*-glucuronide. Moreover, we could successfully separate the (*S*)- and (*R*)-4'-HPPH glucuronide in the improved HPLC condition. In the present study, we sought to determine the catalytic activities for the (*S*)- and

DMD Fast Forward. Published on June 18, 2007 as DOI: 10.1124/dmd.107.015909
This article has not been copyedited and formatted. The final version may differ from this version.

(*R*)-4'-HPPH glucuronide formation by each human UGT enzyme. Recently, we reported that UGT1A enzymes interact with each other, possibly by heterodimerization, changing the kinetics of the enzymatic activity (Fujiwara et al., 2007; Fujiwara et al., submitted). Extending these studies, we investigated the effects of UGT-UGT interaction on the stereoselective formation of 4'-HPPH *O*-glucuronides.

DMD Fast Forward. Published on June 18, 2007 as DOI: 10.1124/dmd.107.015909
This article has not been copyedited and formatted. The final version may differ from this version.

Materials and Methods

Materials. Racemic 5-(4'-hydroxyphenyl)-5-phenylhydantoin (4'-HPPH), UDP-glucuronic acid (UDPGA), and alamethicin were purchased from Sigma-Aldrich (St. Louis, MO). Phenytoin was purchased from Wako Pure Chemicals (Osaka, Japan). Pooled human liver microsomes were from BD Gentest (Woburn, MA). Racemic 4'-HPPH was separated to (*S*)- and (*R*)-enantiomers according to a method by Yasumori et al (1999) using a Chiralcel OJ (4.6 x 250 mm, 10 µm) column (Daicel Chemical, Osaka, Japan). All other chemicals and solvents were of the highest grade commercially available.

Recombinant human UGT and immunoblot analysis

Microsomes from baculovirus-infected insect cells expressing human UGT1A1, UGT1A3, UGT1A4, UGT1A6, UGT1A7, UGT1A8, UGT1A9, UGT1A10, UGT2B4, UGT2B7, UGT2B15, UGT2B17, and CYP2C9 (Supersomes) were from BD Gentest. Single and double expression systems of UGT1A1, UGT1A4, UGT1A6 and UGT1A9 stably expressed in HEK293 cells were previously established in our laboratory (Fujiwara et al., 2007; Fujiwara et al., submitted). For double expression systems, the clones expressing two isoforms almost equally were selected in this study. Total cell homogenates were prepared as described previously (Fujiwara et al., 2007). The expression levels of UGT1A proteins in the homogenates were determined by immunoblot analysis using rabbit anti-human UGT1A polyclonal antibody (BD Gentest), and defined based on a standard curve using the UGT1A1 single expression system (1 unit per 1 mg of cell homogenates), as described previously (Fujiwara et al., 2007).

(*S*)- and (*R*)-4'-HPPH *O*-glucuronide formation. A typical incubation mixture (100 µl total volume) contained 50 mM Tris-HCl buffer (pH 7.4), 5 mM $MgCl_2$, 2.5 mM UDPGA, 25 µg/ml alamethicin, 0.5 mg/ml human liver microsomes or 1 mg/ml recombinant UGTs (single or double expression systems in HEK293 cells, and Supersomes), and racemic 4'-HPPH or

each enantiomer. Since it was confirmed that alamethicin increased the 4'-HPPH *O*-glucuronide formation both in human liver microsomes (2.2 – 2.5 folds) and by recombinant UGTs (1.0 – 1.8 folds), alamethicin was included in all incubation mixtures. 4'-HPPH was dissolved in methanol, and the final concentration of the organic solvent in the incubation mixture was set at 1%. It was confirmed that the inhibitory effects of 1% methanol on 4'-HPPH *O*-glucuronidation were negligible. The reactions were initiated by the addition of UDPGA and were then incubated at 37ºC for 60 min. The reactions were terminated by 100 µl of 10% perchloric acid. After the centrifugation at 10,000 g for 5 min, the supernatant (50 µl) was injected into the HPLC system. HPLC analyses were performed using a PC-980 pump (Jasco, Tokyo, Japan), UV-970 intelligent UV/VIS detector (Jasco), AS-950-10 autosampler (Jasco), D-2500 integrator (Hitachi, Tokyo, Japan), and CTO-6A column oven (Shimadzu, Kyoto, Japan) equipped with an YMC-Pack ODS-AM (4.6 x 150 mm；5 µm）column (YMC, Kyoto, Japan). The mobile phase was 10% acetonitrile/50 mM potassium dihydrogenphosphate. The flow rate was 0.7 ml/min and the column temperature was 35°C. The eluent was monitored at 214 nm with a noise-base clean Uni-3 (Union, Gunma, Japan). The Uni-3 can reduce the noise by integrating the output, increase the signal 3-fold by differentiating the output, and 5-fold by further amplification with an internal amplifier, resulting in a maximum 15-fold amplification of the signal. The retention times of (*R*)- and (*S*)-4'-HPPH *O*-glucuronides and racemic 4'-HPPH were 16.8 min, 17.6 min, and 109 min (Fig. 1A). The detection limit of (*S*)- and (*R*)-4'-HPPH *O*-glucuronides was 0.1 pmol.

Quantification of 4'-HPPH *O*-glucuronides. The incubation mixtures with human liver microsomes including 4'-HPPH *O*-glucuronides were extracted with diethyl ether to exclude the large amount of unconjugated 4'-HPPH. Peak heights of the 4'-HPPH *O*-glucuronides in the residual water phase were determined with the HPLC condition described above (Fig. 1B). 4'-HPPH in the residual water phase was also quantified (Fig. 1D) comparing it with the peak height of the authentic standard (Fig. 1F), using the modified HPLC condition (the mobile phase was 20% acetonitrile/50 mM potassium dihydrogenphosphate and the flow rate was 1

DMD Fast Forward. Published on June 18, 2007 as DOI: 10.1124/dmd.107.015909
This article has not been copyedited and formatted. The final version may differ from this version.

ml/min). The retention time of 4'-HPPH was 13.0 min. A part of the water phase was incubated with 800 U/ml of β-glucuronidase at 37ºC for 24 hr. 4'-HPPH formed by the hydration of glucuronides was quantified (Fig. 1E). Once we determined the peak height per known content of 4'-HPPH *O*-glucuronide, it was applied to the calculation of the 4'-HPPH *O*-glucuronide formed in the incubation mixtures.

Kinetic analyses of (*S*)- and (*R*)-4'-HPPH glucuronide formation. 4'-HPPH glucuronide formation in human liver microsomes and recombinant UGTs was determined with 5 μM to 500 μM racemic 4'-HPPH. To measure the activity in human liver microsomes at 1 mM racemic 4'-HPPH, 2 μl of 50 mM substrate in methanol was added to 100 μl of the incubation mixture, resulting in a 2% methanol concentration. Therefore, the observed activity was corrected with the inhibition percentage (5% for (*S*)-4'-HPPH *O*-glucuronide formation and 12% for (*R*)-4'-HPPH *O*-glucuronide formation). Kinetic parameters were estimated by fitting untransformed experimental data to the Hill equation using a KaleidaGraph computer program (Synergy Software, Reading, PA) designed for nonlinear regression analysis.
The Hill equation, which describes sigmoidal kinetics, is

$$V = \frac{Vmax \times S^n}{S_{50}{}^n + S^n}$$

where V is the velocity of the reaction, S is the substrate concentration, Vmax is the maximum velocity, S_{50} is the substrate concentration showing the half Vmax, and n is the Hill coefficient. Maximum clearance (CLmax), which has been proposed as an appropriate parameter for sigmoid kinetic data instead of intrinsic clearance (Houston and Kenworthy, 2000; Uchaipichat et al., 2004), was calculated by the following equation:

$$CLmax = \frac{Vmax}{S_{50}} \times \frac{(n-1)}{n(n-1)^{1/n}}$$

Data are expressed as mean ± SD of three independent determinations.

Statistical analyses

Statistical significances of the kinetic parameters were determined by analysis of variance (ANOVA) followed by Dunnett's test. A value of $P < 0.05$ was considered statistically significant.

DMD Fast Forward. Published on June 18, 2007 as DOI: 10.1124/dmd.107.015909
This article has not been copyedited and formatted. The final version may differ from this version.

Results

(*S*)- and (*R*)-4'-HPPH *O*-glucuronide formation in human liver microsomes. When the pooled human liver microsomes were incubated with racemic 4'-HPPH and UDPGA, two peaks with retention times of 16.8 min and 17.6 min were observed (Fig. 1A). Both peaks appeared to correspond 4'-HPPH *O*-glucuronide, since these peaks disappeared by treatment with β-glucuronidase. The formation of these glucuronides increased linearly with an incubation time up to 90 min, and with a protein concentration up to 2 mg/ml. To identify which of two peaks corresponds to (*S*)-4'-HPPH *O*-glucuronide, (*S*)-4'-HPPH prepared from the incubation of phenytoin with recombinant CYP2C9 and an NADPH-generating system was used as the substrate. Incubation of the prepared (*S*)-4'-HPPH with the human liver microsomes and UDPGA showed only a peak with the retention time 17.6 min. Accordingly, two peaks at 16.8 min and 17.6 min were determined to correspond to (*R*)- and (*S*)-4'-HPPH *O*-glucuronides, respectively. For the quantification of the 4'-HPPH *O*-glucuronides, the decrease of 4'-HPPH *O*-glucuronides and the increase of 4'-HPPH was compared by the treatment of β-glucuronidase (Table 2). Repetitive estimations with an incubation mixture using racemic 4'-HPPH or each enantiomer as the substrate demonstrated that the peak height of 4'-HPPH *O*-glucuronide per 1 pmol was 881 ± 42 (CV% was 4.8%). These results suggest that the approach to quantify the 4'-HPPH *O*-glucuronides was sufficiently reliable.

Kinetic analyses of the (*S*)- and (*R*)-4'-HPPH *O*-glucuronide formation in the pooled human liver microsomes were performed with racemic 4'-HPPH. The kinetics were fitted to the Hill equations (Fig. 2). The abscissa denotes the concentrations of (*S*)- or (*R*)-4'-HPPH enantiomer, namely half concentrations of racemic 4'-HPPH. For the (*S*)-4'-HPPH *O*-glucuronide formation, S_{50} was 256 ± 30 μM and Vmax was 3.9 ± 0.2 nmol/min/mg, and Hill coefficient, n = 1.3 ± 0.0. For the (*R*)-4'-HPPH *O*-glucuronide formation, S_{50} was 236 ± 17 μM and Vmax was 1.4 ± 0.0 nmol/min/mg, and Hill coefficient, n = 1.5 ± 0.1. Thus, the CLmax of (*S*)-4'-HPPH *O*-glucuronide formation (2.3 ± 0.2 μl/min/mg) was 2.9 fold higher than that of (*R*)-4'-HPPH *O*-glucuronide formation (0.8 ± 0.1 μl/min/mg) in the pooled

human liver microsomes. To investigate whether one enantiomer affects the activity or the sigmoidal kinetics of the other, (*S*)- and (*R*)-4'-HPPH enantiomers were isolated from racemic 4'-HPPH. Although the activities could be measured only up to 50 μM (*S*)- and (*R*)-4'-HPPH enantiomers because of the limited quantity, they were almost the same as the activities with racemic 4'-HPPH at twice the concentration. Therefore, racemic 4'-HPPH was used as the substrate in the subsequent studies.

(*S*)- and (*R*)-4'-HPPH *O*-glucuronide formation by recombinant UGT enzymes.

Recombinant human UGT enzymes expressed in baculovirus-infected insect cells were screened for 4'-HPPH *O*-glucuronide formation. As shown in Fig. 3A, UGT1A1, UGT1A9, and UGT2B15 showed 4'-HPPH *O*-glucuronide formation. UGT1A1 dominantly formed (*R*)-4'-HPPH *O*-glucuronide (43 pmol/min/mg) rather than (*S*)-4'-HPPH *O*-glucuronide (5 pmol/min/mg). In contrast, UGT1A9 and UGT2B15 dominantly formed (*S*)-4'-HPPH *O*-glucuronide (26 and 91 pmol/min/mg, respectively) rather than (*R*)-4'-HPPH *O*-glucuronide (9 and 15 pmol/min/mg, respectively). The HEK293 cell homogenates expressing human UGT1A1, UGT1A4, UGT1A6, and UGT1A9 were also used to determine the 4'-HPPH glucuronidation. UGT1A1 and UGT1A9 selectively formed (*R*)- and (*S*)-4'-HPPH *O*-glucuronides, respectively (Fig. 3B). To normalize the UGT1A expression levels, immunoblot analysis using anti-human UGT1A antibodies was performed. The expression levels of UGT1A1 and UGT1A9 in Supersomes were previously determined to be 15.9 unit/mg and 10.4 unit/mg, respectively (Fujiwara et al., 2007). The expression levels of UGT1A1 and UGT1A9 in HEK293 expression systems were determined to be 1.00 ± 0.03 unit/mg and 0.14 ± 0.02 unit/mg, respectively (Table 1). By the correction of the activity with the UGT1A expression level, the HEK293 expression systems showed higher activity than Supersomes (Figs. 3C, D). In the HEK293 expression systems, the (*S*)- and (*R*)-4'-HPPH *O*-glucuronide formation by UGT1A1 was 4 pmol/min/unit and 36 pmol/min/unit, respectively; the (*S*)- and (*R*)-4'-HPPH *O*-glucuronide formation by UGT1A9 was 51 pmol/min/unit and 10 pmol/min/unit, respectively.

DMD Fast Forward. Published on June 18, 2007 as DOI: 10.1124/dmd.107.015909
This article has not been copyedited and formatted. The final version may differ from this version.

Kinetics of (*S*)- and (*R*)-4'-HPPH *O*-glucuronide formation by recombinant human UGT enzymes. Kinetics analyses of the 4'-HPPH *O*-glucuronide formation by the UGT1A1, UGT1A9, and UGT2B15 Supersomes were performed with racemic 4'-HPPH. All the kinetics were fitted to the Hill equation without the (*R*)-4'-HPPH *O*-glucuronide formation by UGT1A9 (Table 3). UGT1A1 showed an S_{50} of 81 μM and Vmax of 14 pmol/min/mg for (*S*)-4'-HPPH *O*-glucuronide formation, and showed an S_{50} of 110 μM and Vmax of 179 pmol/min/mg for (*R*)-4'-HPPH *O*-glucuronide formation. UGT1A9 showed an S_{50} of 25 μM and Vmax of 38 pmol/min/mg for (*S*)-4'-HPPH *O*-glucuronide formation, and showed an S_{50} of 33 μM and Vmax of 16 pmol/min/mg for (*R*)-4'-HPPH *O*-glucuronide formation. UGT2B15 showed an S_{50} of 91 μM and Vmax of 504 pmol/min/mg for (*S*)-4'-HPPH *O*-glucuronide formation, and showed an S_{50} of 96 μM and Vmax of 121 pmol/min/mg for (*R*)-4'-HPPH *O*-glucuronide formation.

Kinetics analyses of the 4'-HPPH *O*-glucuronide formation by the recombinant UGT1A1 and UGT1A9 in HEK293 cells were also performed with racemic 4'-HPPH. The kinetics were fitted to the Hill equation (Fig. 4, Table 3). UGT1A1 showed an S_{50} of 48 μM and normalized Vmax of 9 pmol/min/unit for (*S*)-4'-HPPH *O*-glucuronide formation, and showed an S_{50} of 74 μM and normalized Vmax of 110 pmol/min/unit for (*R*)-4'-HPPH *O*-glucuronide formation. UGT1A9 showed an S_{50} of 23 μM and normalized Vmax of 67 pmol/min/unit for (*S*)-4'-HPPH *O*-glucuronide formation, and showed an S_{50} of 56 μM and normalized Vmax of 22 pmol/min/unit for (*R*)-4'-HPPH *O*-glucuronide formation.

Effects of coexpression of other UGT1A isoforms on (*S*)- and (*R*)-4'-HPPH *O*-glucuronide formation catalyzed by UGT1A1 or UGT1A9. Double expression systems of human UGT1A in HEK293 cells were used to determine the effects of other isoforms on 4'-HPPH *O*-glucuronide formation catalyzed by UGT1A1 or UGT1A9. The activities of the double expression systems were normalized with the expression levels of UGT1A1 and UGT1A9 proteins summarized in Table 1. Coexpression of UGT1A4 significantly increased

DMD Fast Forward. Published on June 18, 2007 as DOI: 10.1124/dmd.107.015909
This article has not been copyedited and formatted. The final version may differ from this version.

the normalized Vmax values of both (*S*)- and (*R*)-4'-HPPH *O*-glucuronide formation catalyzed by UGT1A1 (Table 3). Coexpression of UGT1A6 increased the S_{50} values and significantly decreased the normalized Vmax values of both (*S*)- and (*R*)-4'-HPPH *O*-glucuronide formation catalyzed UGT1A1. In contrast, coexpression of UGT1A4 decreased the normalized Vmax values or both (*S*)- and (*R*)-4'-HPPH *O*-glucuronide formation catalyzed by UGT1A9. Coexpression of UGT1A6 significantly increased the S_{50} value and decreased the normalized Vmax value of (*S*)-4'-HPPH *O*-glucuronide formation, and decreased the normalized Vmax value of (*R*)-4'-HPPH *O*-glucuronide formation catalyzed by UGT1A9. Thus, coexpression of UGT1A4 showed opposite effects toward UGT1A1- and UGT1A9-catalyzed 4'-HPPH *O*-glucuronide formation, but coexpression of UGT1A6 showed similar effects on UGT1A1- and UGT1A9-catalyzed 4'-HPPH *O*-glucuronide formation. In any case, the UGT-UGT interaction did not alter the stereoselectivity of the 4'-HPPH *O*-glucuronide formation.

The double expression system UGT1A1/UGT1A9 was also used to investigate the interaction of UGT1A1 and UGT1A9 (Fig. 5). Since both isoforms have the catalytic activity toward 4'-HPPH *O*-glucuronide formation, the activity by the double expression system UGT1A1/UGT1A9 was predicted as the sum of activities by UGT1A1 and UGT1A9. For the (*S*)-4'-HPPH *O*-glucuronide formation, the observed activities were lower than the predicted activities based on the expression levels of UGT1A1 and UGT1A9 proteins (Fig. 5). In contrast, for the (*R*)-4'-HPPH *O*-glucuronide formation, the observed activities were higher than the predicted activities at enantiomer concentrations > 25 μM. These results suggested that (*R*)-4'-HPPH *O*-glucuronide formation catalyzed by UGT1A1 may be increased by the coexpression of UGT1A9, and (*S*)-4'-HPPH *O*-glucuronide formation catalyzed by UGT1A9 may conversely be decreased by the coexpression of UGT1A1.

Discussion

It has been demonstrated that some UGT enzymes stereoselectively catalyze glucuronidation (Sten et al., 2006; Bichlmaier et al., 2006; Court et al., 2002; Tougou et al., 2004). In the present study, we characterized different human UGT enzymes for glucuronide formation using racemic 4'-HPPH. We found that UGT1A1 dominantly formed (*R*)-4'-HPPH *O*-glucuronide, but UGT1A9 and UGT2B15 dominantly formed (*S*)-4'-HPPH *O*-glucuronide. In human liver microsomes, the (*S*)-4'-HPPH *O*-glucuronide formation was predominant compared with the (*R*)-4'-HPPH *O*-glucuronide formation. Which UGT isoform has a major contribution to the (*S*)- and (*R*)-4'-HPPH *O*-glucuronide formation in human liver microsomes? To address the issue, the absolute protein levels of each UGT isoform in human liver microsomes should be determined. Alternatively, specific substrates or inhibitors for each UGT isoform can be used to estimate the contribution quantitatively. Unfortunately, lacking a methodology for the quantification of the absolute UGT protein levels beyond UGT1A and UGT2B subfamilies as well as a lack of specific substrates or inhibitors prevent us from accomplishing a quantitative estimation.

Concerning the stereoselectivity, a question is raised whether the preference for the (*S*)- and (*R*)-enantiomers is determined by the binding affinity of substrates or by the rate of transfer of glucuronic acid to the already-bound substrate. The kinetic analyses for UGT1A1 and UGT2B15 activities revealed that the S_{50} values for the two enantiomers differed much less than the corresponding Vmax values (Table 3). On this basis, it appears that the differences in the rate of glucuronic acid transfer to the aglycone are the major determinant of the stereoselectivity. In the case of UGT1A9, both differences in the rate of glucuronic acid transfer to the aglycone and in the affinity of the enzyme for 4'-HPPH enantiomers may be involved.

When the activities normalized with the UGT expression level were compared between two recombinant systems (Fig. 3), the activities by the recombinant UGT1A expressed in the baculovirus-infected insect cells were much lower (one tenth or twentieth) than those by

recombinant UGT1A expressed in HEK293 cells. The phenomenon was not specific for 4'-HPPH *O*-glucuronide formation, because similar results were obtained with other substrates such as estradiol, serotonin, and propofol (data not shown). The differences between the recombinant systems might be due to differences in the membrane environment or lipid components in the host cells. Furthermore, the differences in the post-translational modulation of UGT such as glycosylation or phosphorylation between the insect cells and HEK293 cells might be responsible, since such modulations have been reported to affect the UGT activity (Barbier et al., 2000; Basu et al., 2005).

It has been reported that UGTs form homo- and hetero-dimer or oligomer (Matern et al., 1982; Meech and Mackenzie, 1997, Ghosh et al., 2001; Kurkela et al., 2003). In our recent studies (Fujiwara et al., 2007; Fujiwara et al., submitted), the glucuronidations of a variety of typical substrates were determined using the double expression systems of human UGT1A enzymes in order to investigate the effects of the hetero-dimerization on the enzymatic activity. These previous studies demonstrated that coexpression of other UGT1A isoforms differently changed the kinetics of specific activities depending on the substrates as well as UGT isoforms. Extending our studies, it was found that the coexpression of UGT1A4 and UGT1A6 differently affected the kinetics of the 4'-HPPH *O*-glucuronide formation by UGT1A1 or UGT1A9. Thus, the UGT-UGT interactions, which may also occur in human liver microsomes, affected the kinetics of 4'-HPPH *O*-glucuronide formation. The kinetic analyses revealed sigmoid curves in both (*S*)- and (*R*)-4'-HPPH *O*-glucuronide formation by recombinant UGT1A1 and UGT1A9. The sigmoid curve may indicate positive cooperativity owing to the binding of multiple substrate molecules to a single enzyme active site or the existence of multiple conformations of the enzyme (Cornish-Bowden, 1995). Especially, allosteric effects would be feasible, since UGT forms a dimer or oligomer. It is interesting that the cooperativity was not affected by the coexpression of other isoforms, possibly heterodimerization. The S_{50} values of (*S*)- and (*R*)-4'-HPPH *O*-glucuronide formation in human liver microsomes were unexpectedly higher than those by recombinant UGT enzymes. Although the coexpression of other isoforms substantially increased the Km values for certain

substrates (Fujiwara et al., 2007; Fujiwara et al., submitted), prominent effects on the S_{50} values were not observed in the case of 4'-HPPH. We are also interested in interaction between UGT1A and UGT2B. Double expression systems of UGT1A and UGT2B isoforms are now being constructed in our laboratory to investigate the effects of the interaction on the enzymatic activity. In addition, the possibility cannot be excluded that other enzymes such as CYP might also interact with UGT1A, affecting the kinetics. Further studies will be worth pursuing.

In the present study, we characterized the stereoselective 4'-HPPH *O*-glucuronide formation by human UGT1A1, UGT1A9, and UGT2B15. Furthermore, it was demonstrated that interaction between UGT1A enzymes differently affected the kinetics of (*S*)- and (*R*)-4'-HPPH *O*-glucuronide formation catalyzed by UGT1A1 and UGT1A9, but did not affect the stereoselectivity.

Acknowledgements

We acknowledge Mr. Brent Bell for reviewing the manuscript.

References

Bajpai M, Roskos LK, Shen DD, and Levy RH (1996) Roles of cytochrome P4502C9 and cytochrome P4502C19 in the stereoselective metabolism of phenytoin to its major metabolites. *Drug Metab Dispos* 24: 1401-1403.

Barbier O, Girard C, Breton R, Belanger A, and Hum DW (2000) N-glycosylation and residue 96 are involved in the functional properties of UDP-glucuronosyltransferase enzymes. *Biochemistry* 39: 11540-11552.

Basu NK, Kovarova M, Garza A, Kubota S, Saha T, Mitra PS, Banerjee R, Rivera J, and Owens IS (2005) Phosphorylation of a UDP-glucuronosyltransferase regulates substrate specificity. *Proc Natl Acad Sci USA* 102: 6285-6290.

Bichlmaier I, Siiskonen A, Finel M, and Yli-Kauhaluoma J (2006) Stereochemical sensitivity of the human UDP-glucuronosyltransferases 2B7 and 2B17. *J Med Chem* 49: 1818-1827.

Cornish-Bowden A (1995) *Fundamentals of Enzyme Kinetics*, revised ed. Portland Press, London.

Court MH, Duan SX, Guillemette C, Journault K, Krishnaswamy S, von Moltke LL, and Greenblatt DJ (2002) Stereoselective conjugation of oxazepam by human UDP-glucuronosyltransferases (UGTs): *S*-oxazepam is glucuronidated by UGT2B15, while *R*-oxazepam is glucuronidated by UGT2B7 and UGT1A9. *Drug Metab Dispos* 30: 1257-1265.

Fujiwara R, Nakajima M, Yamanaka H, Nakamura A, Katoh M, Ikushiro S, Sakaki T, and Yokoi T. Effects of coexpression of UGT1A9 on enzymatic activities of human UGT1A isoforms. *Drug Metab Dispos* in press.

Ghosh SS, Sappal BS, Kalpana GV, Lee SW, Chowdhury JR, and Chowdhury NR (2001) Homodimerization of human bilirubin-uridine-diphosphoglucuronate glucuronosyltransferase-1 (UGT1A1) and its functional implications. *J Biol Chem* 276: 42108-42115.

Giancarlo GM, Venkatakrishnan K, Granda BW, von Moltke LL, and Greenblatt DJ (2001) Relative contributions of CYP2C9 and 2C19 to phenytoin 4-hydroxylation in vitro: inhibition by sulfaphenazole, omeprazole, and ticlopidine. *Eur J Clin Pharmacol* 57: 31-36.

Houston JB and Kenworthy KE (2000) In vitro-in vivo scaling of CYP kinetic data not consistent with the classical Michaelis-Menten model. *Drug Metab Dispos* 28: 246-254.

Ieiri I, Goto W, Hirata K, Toshitani A, Imayama S, Ohyama Y, Yamada H, Ohtsubo K, and Higuchi S (1995) Effect of 5-(p-hydroxyphenyl)-5-phenylhydantoin (p-HPPH) enantiomers, major metabolites of phenytoin, on the occurrence of chronic-gingival hyperplasia: *in vivo* and *in vitro* study. *Eur J Clin Pharmacol* 49: 51-56.

Ieiri I, Hirata K, Higuchi S, Kojima K, Ikeda M, Yamada H, and Aoyama T (1992) Pharmacoepidemiological study on adverse reactions of antiepileptic drugs. *Chem Pharm Bull* 40: 1280-1288.

Kim PM and Wells PM (1996) Phenytoin-initiated hydroxyl radical formation: characterization by enhanced salicylate hydroxylation. *Mol Pharmacol* **49:** 172-181.

Kurkela M, Garcia-Horsman JA, Luukkanen L, Morsky S, Taskinen J, Baumann M, Kostiainen R, Hirvonen J, and Finel M (2003) Expression and characterization of recombinant human UDP-glucuronosyltransferases (UGTs). UGT1A9 is more resistant to detergent inhibition than the other UGTs and was purified as an active dimeric enzyme. *J Biol Chem* 278: 3536-3544.

Mackenzie PI, Walter Bock K, Burchell B, Guillemette C, Ikushiro S, Iyanagi T, Miners JO, Owens IS, and Nebert DW (2005) Nomenclature update for the mammalian UDP glycosyltransferase (*UGT*) gene superfamily. *Pharmacogenet Genomics* 15: 677-685.

Matern H, Matern S, and Gerok W (1982) Isolation and characterization of rat liver microsomal UDP-glucuronosyltransferase activity toward chenodeoxycholic acid and testosterone as a single form of enzyme. *J Biol Chem* 257: 7422-7429.

Meech R and Mackenzie PI (1997) UDP-glucuronosyltransferase, the role of the amino terminus in dimerization. *J Biol Chem* 272: 26913-26917.

Nakajima M, Sakata N, Ohashi N, Kume T, and Yokoi T (2002) Involvement of multiple UDP-glucuronosyltransferase 1A isoforms in glucuronidation of 5-(4'-hydroxyphenyl)-5-phenylhydantoin in human liver microsomes. *Drug Metab Dispos* 30: 1250-1256.

Parman T, Chen G and Wells PG (1998) Free radical intermediates of phenytoin and related teratogens. *J Biol Chem* **273:** 25079-25088.

Sten T, Qvisen S, Uutela P, Luukkanen L, Kostiainen R, and Finel M (2006) Prominent but reverse stereoselectivity in propranolol glucuronidation by human UDP-glucuronosyltransferases 1A9 and 1A10. *Drug Metab Dispos* 34: 1488-1494.

Tougou K, Gotou H, Ohno Y, and Nakamura A (2004) Stereoselective glucuronidation and hydroxylation of etodolac by UGT1A9 and CYP2C9 in man. *Xenobiotica* 34: 449-461.

Uchaipichat V, Mackenzie PI, Guo XH, Gardner-Stephen D, Galetin A, Houston JB, Miners JO (2004) Human UDP-glucuronosyltransferases: isoform selectivity and kinetics of 4-methylumbelliferone and 1-naphthol glucuronidation, effects of organic solvents, and inhibition by diclofenac and probenecid. *Drug Metab Dispos* 32: 413-423.

Yamanaka H, Nakajima M, Hara Y, Katoh M, Tachibana O, Yamashita J, and Yokoi T (2005) Urinary excretion of phenytoin metabolites, 5-(4'-hydroxyphenyl)-5-phenylhydantoin and its *O*-glucuronide in humans and analysis of genetic polymorphisms of UDP-glucuronosyltransferases. *Drug Metab Pharmacokinet* 20: 135-143.

Yasumori T, Chen LS, Li QH, Ueda M, Tsuzuki T, Goldstein JA, Kato R, and Yamazoe Y (1999) Human CYP2C-mediated stereoselective phenytoin hydroxylation in Japanese: difference in chiral preference of CYP2C9 and CYP2C19. *Biochem Pharmacol* 57: 1297-1303.

Footnote

Hiroyuki Yamanaka is supported as a Research Fellow of the Japan Society for the Promotion of Science.

Submitted paper

Fujiwara R, Nakajima M, Yamanaka H, Katoh M, and Yokoi T. Interactions between human UGT1A1, UGT1A4, and UGT1A6 affect their enzymatic activities.

DMD Fast Forward. Published on June 18, 2007 as DOI: 10.1124/dmd.107.015909
This article has not been copyedited and formatted. The final version may differ from this version.

Figure legends

Fig. 1. Representative chromatogram of HPLC analysis of the (*S*)- and (*R*)-4'-HPPH *O*-glucuronide formation from racemic 4'-HPPH in human liver microsomes. Pooled human liver microsomes (0.5 mg/ml) were incubated with 100 μM racemic 4'-HPPH and 2.5 mM UDPGA at 37°C for 60 min (A). To quantify the 4'-HPPH *O*-glucuronides, the incubation mixtures with human liver microsomes including 4'-HPPH *O*-glucuronides were treated with β-glucuronidase. Chromatograms to detect the 4'-HPPH *O*-glucuronides in the mixture treated with (C) and without (B) the β-glucuronidase. Chromatograms to detect the 4'-HPPH in the mixture treated with (E) and without (D) the β-glucuronidase. Chromatogram of the authentic standard of racemic 4'-HPPH (F).

Fig. 2. Kinetic analyses of (*S*)- and (*R*)-4'-HPPH *O*-glucuronide formation in human liver microsomes. The substrate-velocity curve (A) and Eadie-Hofstee plot (B) of the 4'-HPPH *O*-glucuronide formation are shown. Pooled human liver microsomes were incubated with 5 μM – 1 mM racemic 4'-HPPH and 2.5 mM UDPGA at 37°C for 60 min. The abscissa denotes the concentrations of (*S*)- and (*R*)-4'-HPPH enantiomer, namely the half concentrations of racemic 4'-HPPH. Closed and open circles showed the (*S*)- and (*R*)-4'-HPPH *O*-glucuronide formation from racemic 4'-HPPH, respectively. Closed and open triangles show the (*S*)- and (*R*)-4'-HPPH *O*-glucuronide formation from (*S*)- and (*R*)-4'-HPPH enantiomers, respectively. Since the quantity of 4'-HPPH enantiomers was limited, the activities could be measured only up to a 50 μM substrate concentration. Each data point represents the mean of three independent experiments.

Fig. 3. (*S*)- and (*R*)-4'-HPPH *O*-glucuronide formation by recombinant human UGT enzymes expressed in baculovirus infected insect cells (Supersomes) (A, C) or HEK293 cells (B, D). The activity was expressed as pmol/min/mg (A, B) or pmol/min/unit (C, D). Each recombinant UGT (1 mg/ml) was incubated with 100 μM racemic 4'-HPPH and 2.5 mM

UDPGA at 37°C for 60 min. Closed and open columns show the (*S*)- and (*R*)-4'-HPPH *O*-glucuronide formation, respectively. Each column represents the mean of duplicate determinations. ND: not detected.

Fig. 4. Kinetic analyses of (*S*)- and (*R*)-4'-HPPH *O*-glucuronide formation by recombinant human UGT1A1 (A, B) and UGT1A9 (C, D) in HEK293 cells. The substrate-velocity curve (A, C) and Eadie-Hofstee plot (B, D) of the 4'-HPPH *O*-glucuronide formation are shown. Recombinant UGT1As (1 mg/ml) were incubated with racemic 4'-HPPH (5 - 500 μM) and 2.5 mM UDPGA at 37°C for 60 min. Closed and open circles show the (*S*)- and (*R*)-4'-HPPH *O*-glucuronide formation, respectively. Each data point represents the mean of triplicate determinations.

Fig. 5. Kinetic analyses of (*S*)- and (*R*)-4'-HPPH *O*-glucuronide formation by a double expression system of UGT1A1/UGT1A9. Recombinant UGT1As (1 mg/ml) were incubated with racemic 4'-HPPH (5 - 500 μM) and 2.5 mM UDPGA at 37°C for 60 min. Solid and dashed lines indicated the observed and predicted activities. Closed and open symbols show the (*S*)- and (*R*)-4'-HPPH *O*-glucuronide formation, respectively. Each data point represents the mean of triplicate determinations.

DMD Fast Forward. Published on June 18, 2007 as DOI: 10.1124/dmd.107.015909
This article has not been copyedited and formatted. The final version may differ from this version.

Table 1. Expression levels of each UGT1A protein in double expression systems.

	UGT1A1	UGT1A4	UGT1A6	UGT1A9
		unit/mg		
UGT1A1	1.00 ± 0.03			
UGT1A4		0.74 ± 0.01		
UGT1A6			0.09 ± 0.01	
UGT1A9				0.14 ± 0.02
UGT1A1/1A4	0.62 ± 0.02	0.62 ± 0.03		
UGT1A1/1A6	0.62 ± 0.03		0.69 ± 0.03	
UGT1A1/1A9	0.36 ± 0.01			0.26 ± 0.01
UGT1A4/1A9		0.29 ± 0.02		0.24 ± 0.02
UGT1A6/1A9			0.27 ± 0.01	0.30 ± 0.00

Data are mean ± SD (n = 3).

Table 2. Quantification of 4'-HPPH *O*-glucuronide.

Substrate	Volume of analyte	Hydrolyze (-)				Hydrolyze (+)			4'-HPPH formed by hydration of glucuronides (C–B)	Peak height of glucuronide per 1 pmol A/(C – B)
		4'-HPPH *O*-glucuronide			4'-HPPH (B)	4'-HPPH *O*-glucuronide		4'-HPPH (C)		
		(*S*)-Glucuronide	(*R*)-Glucuronide	Sum of (*S*)- and (*R*)-glucuronides (A)		(*S*)-Glucuronide	(*R*)-Glucuronide			
	µl		*Height*		*pmol*	*height*		*pmol*	*pmol*	*height*
Racemic 4'-HPPH	50	456181	299242	755423	34.8	ND	ND	852.9	818.1	923
(500 µM)	25	223114	145859	368973	11.3	ND	ND	424.8	413.4	892
	5	46160	27310	73470	4.6	ND	ND	84.9	80.4	915
(*S*)-4'-HPPH (50 µM)	50	109600	ND	109600	5.6	ND	ND	138.4	132.8	825
(*R*)-4'-HPPH (50 µM)	50	ND	69990	69990	5.2	ND	ND	87.6	82.4	850
										881 ± 4 (mean ± SD)

ND: Not detected.

Incubation mixture (100 µl) with human liver microsomes and racemic 4'-HPPH (500 µM) or 4'-HPPH enantiomers (50 µM) were extracted with diethyl ether to exclude the large amount of unconjugated 4'-HPPH. The residual water phase was divided into two parts, and one was incubated with β-glucuronidase at 37ºC for 24 hr and the others were incubated without β-glucuronidase. After the removal of protein, aliquots of the incubation mixtures were subjected to HPLC to determine the peak heights of 4'-HPPH *O*-glucuronides and content of 4'-HPPH. Comparing the decreased peak heights of 4'-HPPH *O*-glucuronides with the increased 4'-HPPH by the treatment of β-glucuronidase, the peak height per 1 pmol 4'-HPPH *O*-glucuronide was determined.

Table 3. Kinetic parameters of 4'-HPPH *O*-glucuronidation by recombinant human UGT enzymes.

	(*S*)-4'-HPPH *O*-glucuronide formation					(*R*)-4'-HPPH *O*-glucuronide formation				
	S50	Vmax	Normalized Vmax	CLmax	n	S50	Vmax	Normalized Vmax	CLmax	n
	μM	*pmol/min/mg*	*pmol/min/unit*	*nl/min/unit*		*μM*	*pmol/min/mg*	*pmol/min/unit*	*nl/min/unit*	
UGT1A1 Supersomes	81 ± 20	14 ± 1	1 ± 0	6 ± 1	1.4 ± 0.1	110 ± 27	179 ± 25	11 ± 2	55 ± 4	1.6 ± 0.3
UGT1A9 Supersomes	25 ± 1	38 ± 1	4 ± 0	91 ± 1	1.3 ± 0.0	33 ± 4	16 ± 1	2 ± 0	46 ± 3 [b]	1.0 ± 0.1
UGT2B15 Supersomes	91 ± 12	504 ± 55	NA	NA	1.7 ± 0.1	96 ± 6	121 ± 19	NA	NA	2.2 ± 0.1
[a] UGT1A1	48 ± 5	9 ± 0	9 ± 0	23 ± 2	1.8 ± 0.2	74 ± 12	110 ± 5	110 ± 5	194 ± 20	1.6 ± 0.2
[a] UGT1A1/1A4	49 ± 1	7 ± 0	12 ± 0**	30 ± 1**	1.8 ± 0.2	70 ± 5	86 ± 3	138 ± 5**	250 ± 6**	1.7 ± 0.2
[a] UGT1A1/1A6	66 ± 2*	3 ± 0	4 ± 0**	10 ± 1**	1.7 ± 0.4	91 ± 14	35 ± 4	56 ± 6**	81 ± 6**	1.6 ± 0.2
[a] UGT1A9	23 ± 2	9 ± 1	67 ± 9	382 ± 16	1.5 ± 0.1	56 ± 14	3 ± 0	22 ± 3	56 ± 7	1.5 ± 0.4
[a] UGT1A4/1A9	22 ± 2	12 ± 2	52 ± 8	296 ± 28†	1.7 ± 0.1	41 ± 6	4 ± 1	15 ± 2†	50 ± 11	1.6 ± 0.2
[a] UGT1A6/1A9	35 ± 5††	15 ± 1	50 ± 4†	192 ± 18††	1.5 ± 0.1	54 ± 8	4 ± 1	14 ± 2†	35 ± 2†	1.5 ± 0.2

Data are mean ± SD (n = 3). NA: Not available.

[a] HEK293 expression systems that were established in our previous study (Fujiwara et al., 2007).

[b] The intrinsic clearance (Vmax/Km) was calculated, since the kinetics was fitted to Michaelis-Menten equation.

* $P < 0.05$ and ** $P < 0.01$, compared with single expression system of UGT1A1 in HEK293 cells.

† $P < 0.05$ and †† $P < 0.01$, compared with single expression system of UGT1A9 in HEK293 cells.

DMD Fast Forward. Published on June 18, 2007 as DOI: 10.1124/dmd.107.015909
This article has not been copyedited and formatted. The final version may differ from this version.

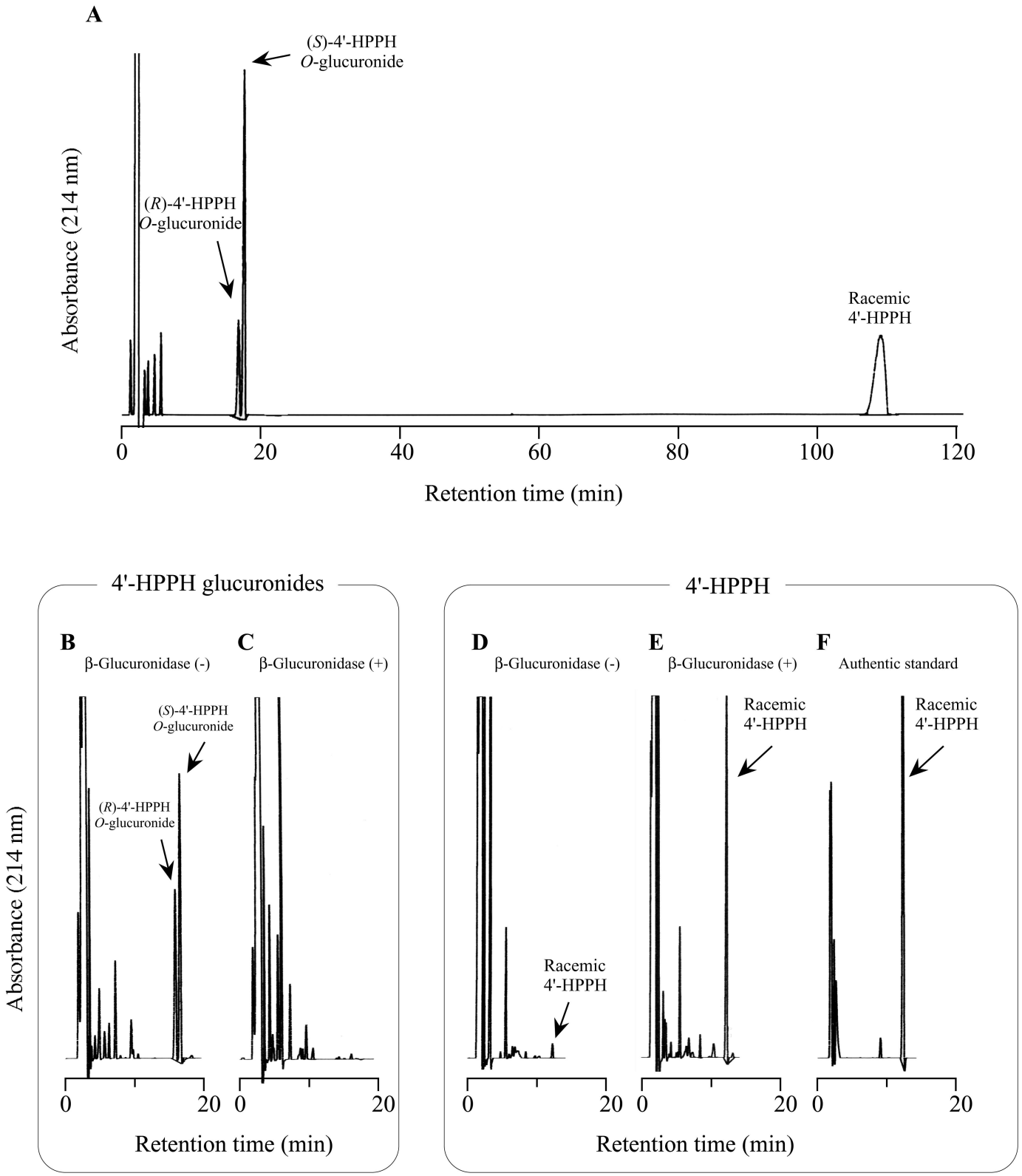

Fig. 2.

DMD Fast Forward. Published on June 18, 2007 as DOI: 10.1124/dmd.107.015909
This article has not been copyedited and formatted. The final version may differ from this version.

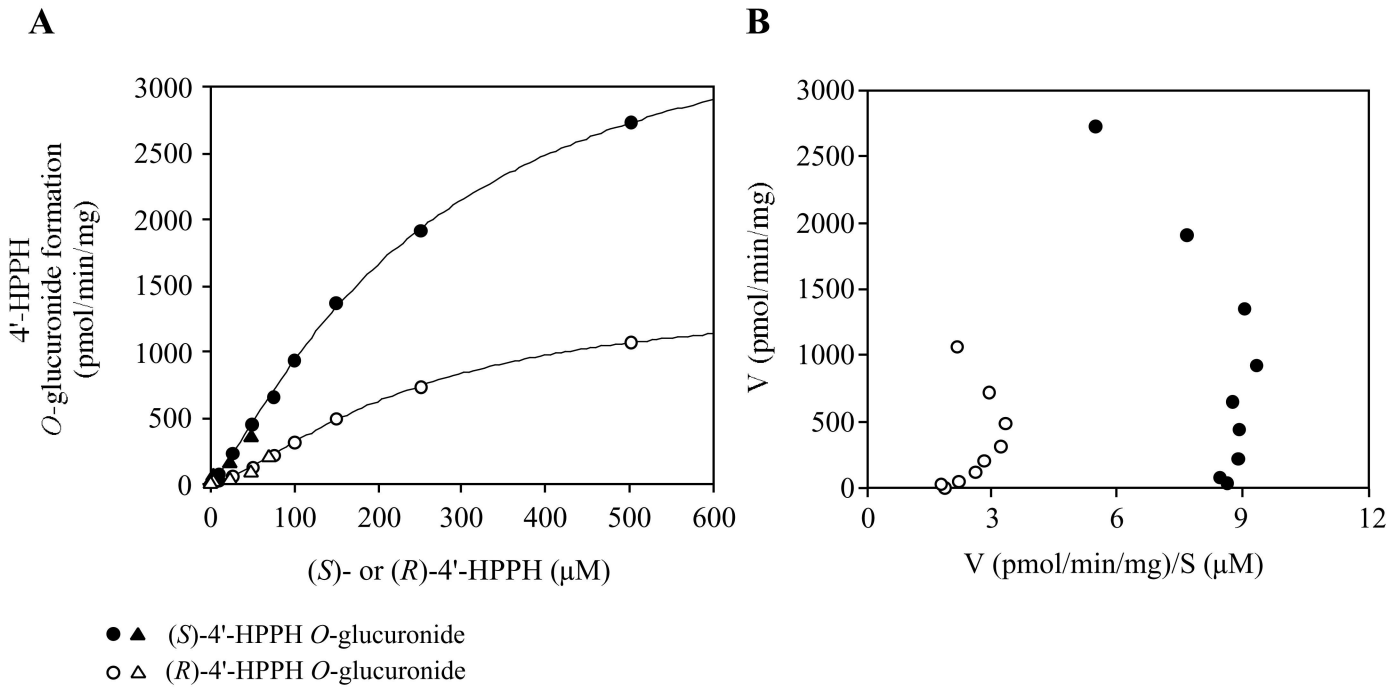

DMD Fast Forward. Published on June 18, 2007 as DOI: 10.1124/dmd.107.015909
This article has not been copyedited and formatted. The final version may differ from this version.

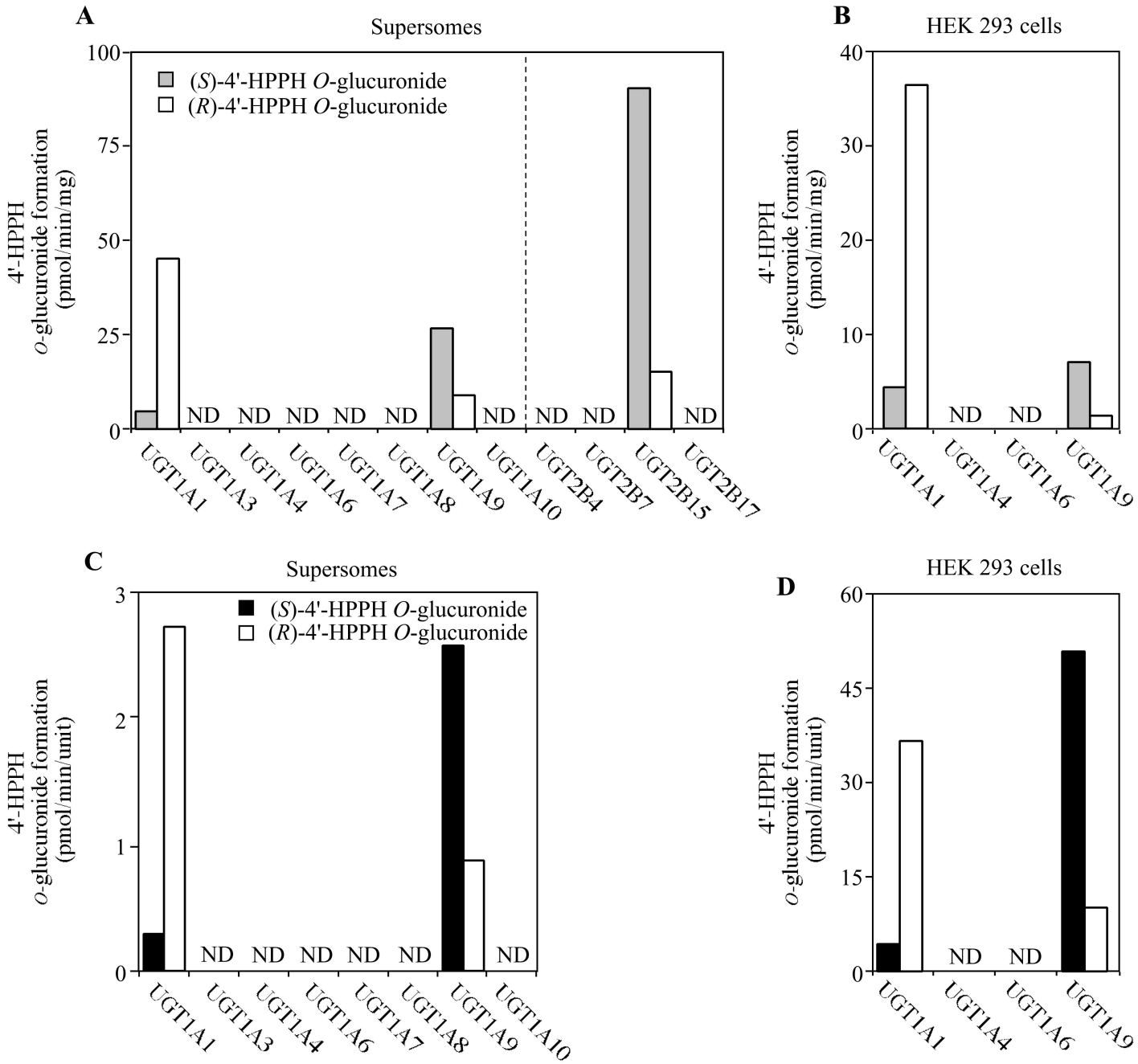

Fig. 4.

DMD Fast Forward. Published on June 18, 2007 as DOI: 10.1124/dmd.107.015909
This article has not been copyedited and formatted. The final version may differ from this version.

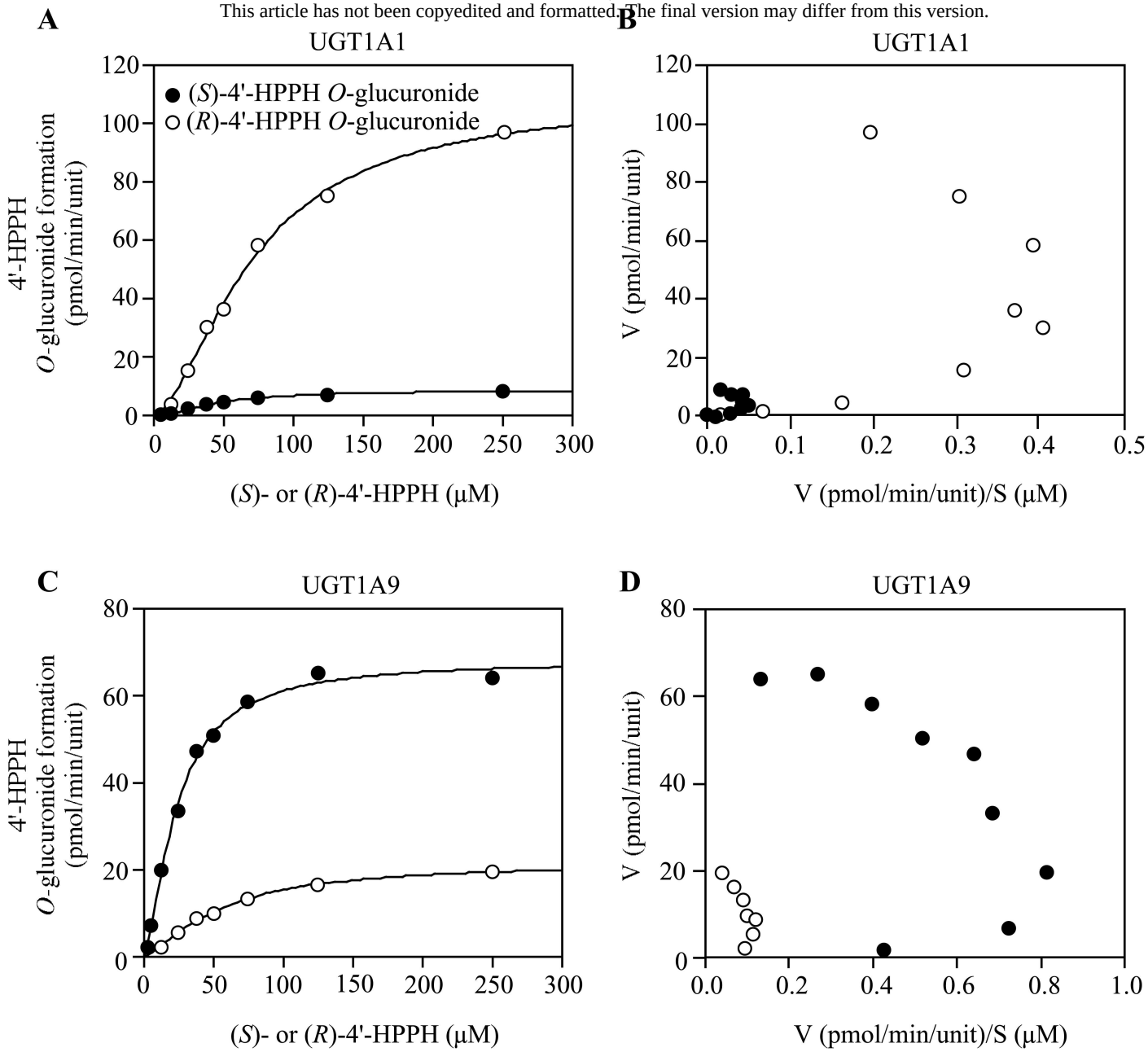

Fig. 5

DMD Fast Forward. Published on June 18, 2007 as DOI: 10.1124/dmd.107.015909